Available online at www.sciencedirect.com
ScienceDirect
Trans. Nonferrous Met. Soc. China 32(2022) 2727−2735
Transactions of Nonferrous Metals Society of China
www.tnmsc.cn

Penetration behavior of electrolyte into graphite cathode in NaF−KF−LiF−AlF_3 system with low cryolite ratios

Bing-xu CHEN, Jian-ping PENG, Yao-wu WANG, Yue-zhong DI

School of Metallurgy, Northeastern University, Shenyang 110819, China

Received 12 July 2021; accepted 8 December 2021

Abstract: The current study focuses on the electrolyte penetration of the graphite cathode in a NaF−KF−LiF−AlF_3 aluminum-electrolysis system with a cryolite ratio of 1.3. It involves a comprehensive investigation of the electrolyte in the cathode before and after electrolysis by X-ray diffraction and analysis of the results by semi-quantitative calculation in MAUD. The results show that KF can promote electrolyte penetration, with higher KF contents resulting in greater penetration. During electrolyte penetration, K_2NaAlF_6 and solid solutions containing KF play important roles in KF-containing systems. LiF effectively prevents the electrolyte penetration, while the $Na_3Li_3Al_2F_{12}$ phase plays an essential role in systems with high LiF contents.

Key words: aluminum electrolysis; KF; LiF; cathode penetration; electrolyte composition; low cryolite ratio

1 Introduction

The aluminum industry is essential to the national economy of China [1]. The commercial electrolyte system currently used for aluminum electrolysis, i.e., Na_3AlF_6−AlF_3 system with a cryolite ratio of 2.6, requires high-temperature conditions, which results in a significant energy and resource burden as well as environmental concerns. Accordingly, low cryolite ratio NaF/KF−AlF_3 systems have been developed to address these issues. For instance, SLEPPY and COCHRAN [2] used NaF−AlF_3 systems with cryolite ratios between 0.65 and 0.80 to achieve aluminum electrolysis below 900 °C [2]. Although improvements in terms of higher current efficiency and lower carbon consumption were obtained, the system was subjected to problems associated with lower alumina solution rates, lower electrical conductivity, and carbon dusting at low alumina contents.

To improve upon this low-cryolite-ratio NaF−AlF_3 system, novel electrolytic systems such as KF−AlF_3 system, LiF−AlF_3 system, NaF−KF−AlF_3 system, and NaF−LiF−AlF_3 system have been developed. The physicochemical characteristics, electrolysis conditions, and alkaline metal penetration of low-cryolite-ratio systems have been studied extensively [3−11]. Nevertheless, the addition of KF reduces conductivity, while the addition of LiF reduces alumina solubility. However, the addition of KF and LiF in combination substantially ameliorates the disadvantages of low-temperature systems. Accordingly, such low-cryolite-ratio systems are being explored as a potential means of aluminum electrolysis.

Research into the cathode penetration behavior of such systems has hitherto been largely focused on alkaline penetration rather than electrolyte penetration. Accordingly, electrolyte composition and its cathode penetration remain relatively under-researched. Cathode penetration causes cathode damage, decreasing cell service life. Therefore, study of this phenomenon is important

Corresponding author: Jian-ping PENG, Tel: +86-24-83680508, E-mail: pengjp@mail.neu.edu.cn
DOI: 10.1016/S1003-6326(22)65979-X

for the aluminum electrolysis industry.

Following the Na penetration, the electrolyte penetrates the graphite cathode. The graphite cathode is not penetrated by pure cryolite melt or liquid aluminum. Rather, electrolyte penetration occurs when aluminum is dissolved in the cryolite melt and penetrates the pores of the graphite cathode [12]. Furthermore, the NaF, KF, or LiF discharge reactions on the cathode or Al replacement reactions in the melt are capable of producing Na, K, or Li, as shown in Reaction (1) [13]. These reactions contribute to corrosion and flaking of the cathode.

$$Al+3NaF/KF/LiF\rightarrow 3Na/K/Li+AlF_3 \quad (1)$$

The studies cited above were concerned with the penetration behavior and chemical reactions of $NaF-AlF_3$ systems. They involved a thorough study by laboratory electrolysis for a short period or spent cathode analysis after prolonged usage. However, the $NaF-KF/LiF-AlF_3$ system has received little attention. LIU et al [14] reported that KF promotes corrosion of the carbon cathode in $KF-AlF_3$ systems through electrochemical analysis. ZHANG et al [15] studied the penetration behavior of $Na_3AlF_6-Al_2O_3-AlF_3$ systems containing LiF and KF, concluding that LiF effectively prevents the alkaline metal damage. Nevertheless, the penetration behavior of $NaF-KF-LiF-AlF_3$-based systems has yet to be fully understood.

Previous work has demonstrated that $NaF-KF-LiF-AlF_3$ systems with low cryolite ratios present an excellent option for aluminum electrolysis due to their modest liquidus region, low electrolysis temperature, and the fact that the molecular ratio does not vary dramatically during electrolysis [7,16,17]. Accordingly, in the current study, the effects of KF and LiF concentration on cathode corrosion were investigated as well as the relationship between electrolyte compositions and cathode corrosion. A more complete understanding of the effects of electrolyte penetration on cathode corrosion will inform strategies to control it and thus increase the service life of aluminum electrolysis cells.

2 Experimental

2.1 Chemicals

Na_3AlF_6 (99%), KF (99%), LiF (99%), AlF_3 (98%), and α-Al_2O_3 (99%) (Sinopharm Chemical Reagent Co., Ltd.) were used to prepare the electrolyte. The specific preparation method was previously reported [16].

2.2 Electrolysis experiment

Constant-current electrolysis was conducted using a two-graphite-electrode setup at 800 °C with an electrolysis duration of 2 h. An Ar atmosphere was utilized to prevent oxidation of the samples and the steel parts of the apparatus. The cathode and anode samples were cut into cylindrical specimens of d52 mm × 40 mm and d30 mm × 50 mm, respectively. The conductor was a stainless-steel bar that also served as a guide bar. An Al_2O_3 tube was inserted into the top of the cathode, which was coated with BN to ensure direct current across the cathode. The anode–cathode distance (ACD) was 4 cm. A cathode current density of 0.6 A/cm^2 was supplied by a digital DC regulated power supply (MES−30100, Suzhou, China), and the voltage vs time profiles were recorded using an Agilent 34401A multimeter. Additionally, alumina was added to the molten salts to maintain the alumina content of the electrolyte.

2.3 Electrolyte sample preparation

According to a previous study, calcination can have an effect on the final results of electrolyte analysis [16]. Accordingly, a different sample preparation procedure to that previously reported was utilized to acquire electrolytes without calcination at high temperatures. The general procedure was similar to that described in Section 2.2. The main difference was that the cathode had a recess on the vertical axis (d5 mm × 15 mm) for collecting electrolytes (Fig. 1). Cryolite ratio (CR) was defined as $CR=x(NaF+KF+LiF)/x(AlF_3)$.

2.4 Sample characterization

The cathode without recess was cut into several 5 mm slices, and the composition of the penetrated electrolyte was determined quantitatively by the ash method and the X-ray diffraction (XRD) [12]. X-ray powder diffraction patterns were obtained using a PANalytical x'Pert Pro MRD with Cu K_α radiation from 10° to 70° at a scan speed of 0.067 (°)/s. The specific compositions were obtained by analyzing the data using semi-quantitative calculation in MAUD. In this process,

samples obtained from a $NaF-AlF_3$ system with a cryolite ratio of 1.3 were analyzed to establish the precision of the method. Relative to the theoretical mass fractions for $Na_5Al_3F_{14}$ and AlF_3, the errors were 0.3% and 2.2%, respectively, which are within experimental limits (5%). The results were mainly utilized to illustrate the bath's percolation in the concentration profiles.

3 Results and discussion

3.1 Mass gain of graphite cathode during electrolysis

Figure 2 shows the mass gain for graphite cathodes electrolyzed in various systems and at different depths. Under electrolyzing conditions, the

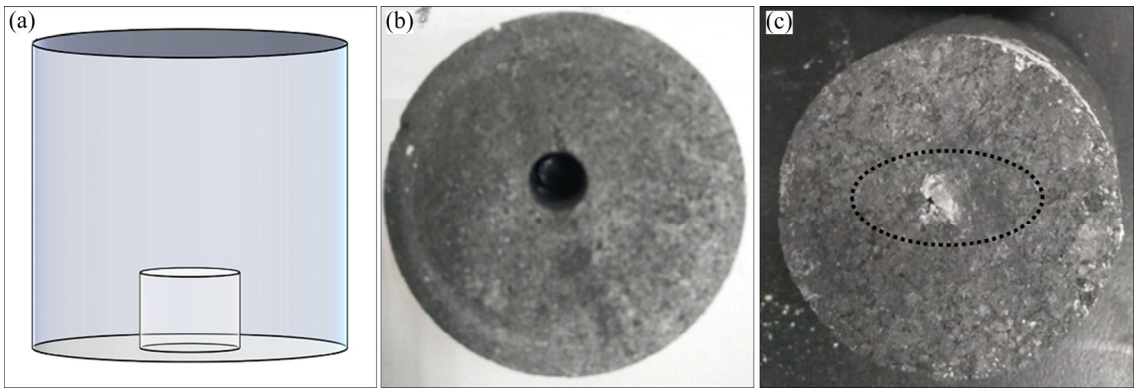

Fig. 1 Electrolyte penetration into cathode: (a) Schematic of cathode showing position of recess; (b, c) Photographic images of cathode before (b) and after (c) electrolysis

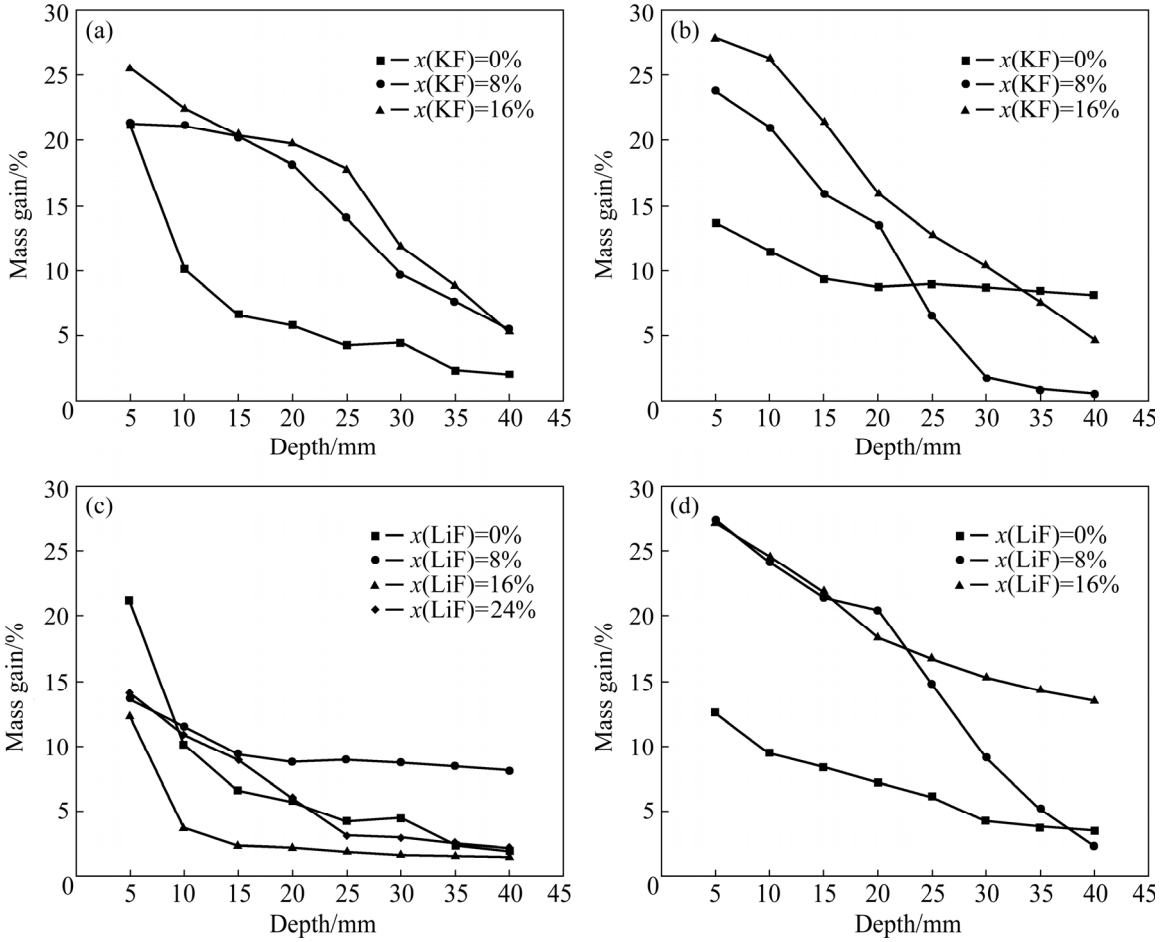

Fig. 2 Mass gain for graphite cathodes during electrolysis in $NaF-KF-LiF-AlF_3$ systems: (a) $NaF-KF-AlF_3$ system; (b) $NaF-KF-8\%LiF-AlF_3$ system; (c) $NaF-LiF-AlF_3$ system; (d) $NaF-4\%KF-LiF-AlF_3$ system

molten salt is partially reduced and penetrates the cathode surface. As a result, as illustrated in Fig. 2, an extremely steep electrolyte gradient exists between the top and bottom of the reactor. Thus, the mass gain of graphite varies depending on the LiF and KF concentrations of the electrolytes.

The mass gain increases with increasing KF content, as shown in Figs. 2(a) and (b). Compared with these figures, there are some minor differences in Figs. 2(c) and (d). It can be observed that increasing LiF content in the system without KF causes a significant drop-off (Fig. 2(c)), with this trend also observed for the system containing 4% KF (Fig. 2(d)) but to a lesser extent. These differences can be attributed to the alkaline metal and electrolyte penetration behavior.

As previously reported, alkaline-metal generation is the predominant cathode reaction during electrolysis [3,14,18]. The alkaline metals (Na, K and Li) generated as an electrolysis by-product diffuse into the carbon block and form an alkaline–graphite intercalation compound. Importantly, the K-graphite intercalation compound (K−GIC) contributes to electrolyte penetration behavior [14,19]. Unlike K−GIC, the Li−graphite intercalation compound is non-layered [15]. Thus, the reaction of Li with graphite mainly occurs on the graphite surface and inhibits the penetration of other alkaline metals.

Aside from ameliorating Na and K penetration, the presence of LiF inhibits the wettability of the electrolyte melt for the carbon cathode, also hindering electrolyte penetration [15]. Thus, the highest electrolyte content is observed for the top of the cathode, while the electrolyte content in the remaining areas is lower in systems with LiF.

Figure 3 shows the SEM images of cathode samples taken 10 cm from the top of the cathode

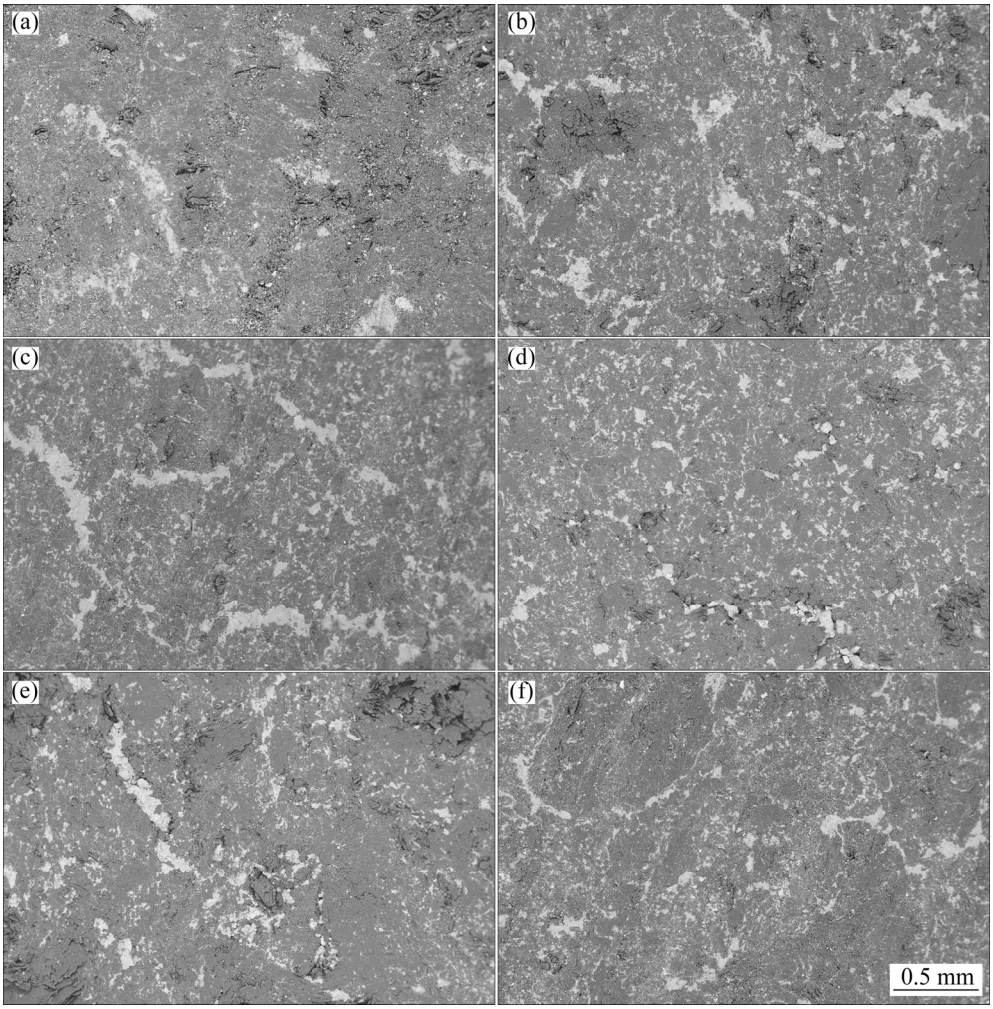

Fig. 3 SEM images of cathode samples after electrolysis in different systems at same depth: (a−c) $NaF−AlF_3$ systems with x(KF)=0 (a), x(KF)=8% (b) and x(KF)=16% (c); (d−f) $NaF−4\%KF−AlF_3$ systems with x(LiF)=0 (d), x(LiF)=8% (e) and x(LiF)=16% (f)

after electrolysis in different systems. Figures 3(a−c) clearly show that KF promotes electrolyte permeation as the white area increases with the increase of KF content and some electrolyte accumulates. In contrast, Figs. 3(d−f) show that the electrolyte aggregation phenomenon is decreased and the white area is weakened, indicating that LiF inhibits electrolyte penetration. This phenomenon is also consistent with the results shown in Fig. 2.

3.2 Analysis of electrolytes inside graphite cathode during electrolysis

The electrolyte samples were obtained on the basis of Section 2.3 to identify the predominant electrolytes inside the graphite cathodes, and the analysis results are shown in Table 1 and Fig. 4. The solidified electrolytes for low KF and LiF concentrations contain mainly Na_3AlF_6 and $Na_5Al_3F_{14}$. The $Na_5Al_3F_{14}$ phase is the main component in the electrolyte. $Na_5Al_3F_{14}$ has been shown to form solid solutions ($(Na_{(5-x)}K_x)Al_3F_{14}$) in the limited range of $0<x<0.4$ [20]. In a previous study, a NaF−KF−AlF_3 system with a low LiF content was also observed to form a $Na_5Al_3F_{14}$ solid solution containing LiF [16]. Accordingly, K and Li compounds are not detected.

The presence of Na_3AlF_6 could be due to the change of cryolite ratio on the cathode surface. In the process of electrolysis, the cryolite ratio of the electrolyte melt is increased by the accumulation of NaF on the cathode surface. As the LiF content in the electrolyte gradually increases, some LiF penetrates to the cathode with the electrolyte, and the LiF content exceeds the concentration of the

Table 1 Electrolyte analysis results for 1.3NaF−KF− LiF−AlF_3 system

System	After electrolysis	Before electrolysis
x(KF)=0, x(LiF)=0	$Na_5Al_3F_{14}$, Na_3AlF_6	$Na_5Al_3F_{14}$, AlF_3
x(KF)=4%, x(LiF)=8%	$Na_5Al_3F_{14}$, Na_3AlF_6	$Na_5Al_3F_{14}$, AlF_3
x(KF)=16%, x(LiF)=0	Na_3AlF_6, $K_2NaAl_3F_{12}$, K_2NaAlF_6	$Na_5Al_3F_{14}$, $K_2NaAl_3F_{12}$
x(KF)=16%, x(LiF)=8%	Na_3AlF_6, $Na_5Al_3F_{14}$, $K_2NaAl_3F_{12}$, $Na_3Li_3Al_2F_{12}$, K_2NaAlF_6	$Na_5Al_3F_{14}$, $K_2NaAl_3F_{12}$, $Na_3Li_3Al_2F_{12}$, K_2NaAlF_6
x(KF)=4%, x(LiF)=16%	$Na_5Al_3F_{14}$, AlF_3, $Na_3Li_3Al_2F_{12}$ K_2LiAlF_6, Unknown(trace)	$Na_5Al_3F_{14}$, AlF_3, $Na_3Li_3Al_2F_{12}$

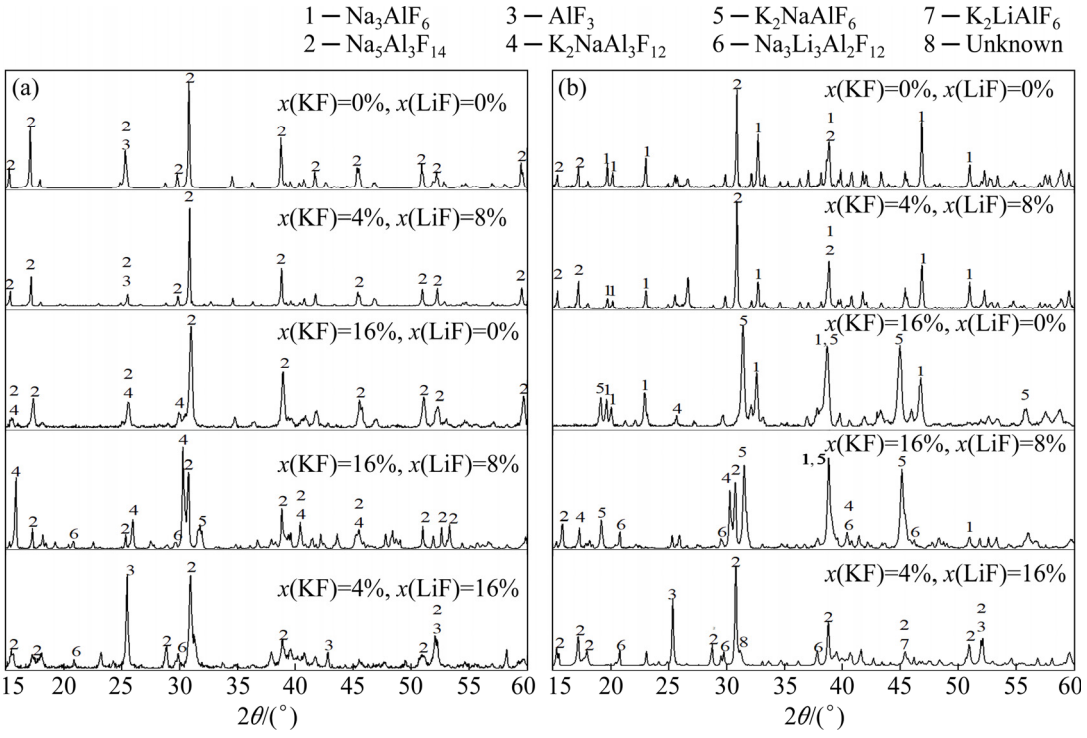

Fig. 4 XRD patterns of electrolytes in different systems before (a) and after (b) electrolysis

dilute solution, forming Li compounds. Li mainly forms solid solutions with chiolite and cryolite. The content of NaF gradually decreases as the content of LiF increases, and the cryolite content decreases accordingly. Thus, Li compounds instead of solid solutions are formed.

The formation of K compounds is similar, in that when the KF and LiF contents increase, K and Li compounds, respectively, are generated in the electrolyte. Therefore, K and Li compounds, including $K_2NaAl_3F_{12}$, K_2NaAlF_6, $Na_3Li_3Al_2F_{12}$, and K_2LiAlF_6 are detected with increasing KF and LiF contents. In addition to the electrolyte being an unknown phase, the peak position occurs in the range $0.4<x(\text{LiF})/x(\text{NaF+LiF})<0.7$ for the 1.3NaF−LiF−AlF_3 system.

3.3 Graphite penetration pathway during electrolysis

3.3.1 Effects of KF content on mass gain for graphite cathodes

As shown in Fig. 5, the electrolyte for the Na_3AlF_6−KF−AlF_3 system is composed of Na_3AlF_6, K_2NaAlF_6, and two types of alumina. Quantitative XRD analyses reveal that the Na_3AlF_6 content significantly decreases as the KF content increases. In this system, high KF contents result in a decrease in Na_3AlF_6 production.

Correspondingly, the K_2NaAlF_6 content increases with increasing KF content for the same depth, as shown in Fig. 5(b). However, unlike the decreasing trend for the Na_3AlF_6 phase, the content of K_2NaAlF_6 increases with increasing depth. The specific explanation for this is given in Section 3.2.

It should be noted that the electrolyte compositions here are different from those given in Table 1. The $K_2NaAl_3F_{12}$ phase cannot be detected after calcination. This may be due to two main reasons: Firstly, at temperatures higher than 580 °C, $K_2NaAl_3F_{12}$ becomes highly volatile and is prone to react with air moisture and form two further phases, i.e., K_2NaAlF_6 and Al_2OF_4 [21]; secondly, with increasing KF content, the K_2NaAlF_6 phase becomes the dominant compound instead of $K_2NaAl_3F_{12}$ [3,10]. Thus, the presence of K_2NaAlF_6 is basically in line with the results.

Figure 5(c) shows that there are two types of alumina in the cathode. The α-Al_2O_3 content gradually decreases as the η-Al_2O_3 content increases with increasing KF content. When x(KF)=16%, α-Al_2O_3 is almost entirely converted to η-Al_2O_3. This phenomenon is consistent with the conclusions obtained by FOSTER [22], i.e., $x(AlF_3)>25\%$ in the Na_3AlF_6−AlF_3 system promotes the conversion of α-Al_2O_3 into η-Al_2O_3. Furthermore, the presence of KF may promote the transformation of α-Al_2O_3 to η-Al_2O_3, and its transformation is accelerated with increasing KF content.

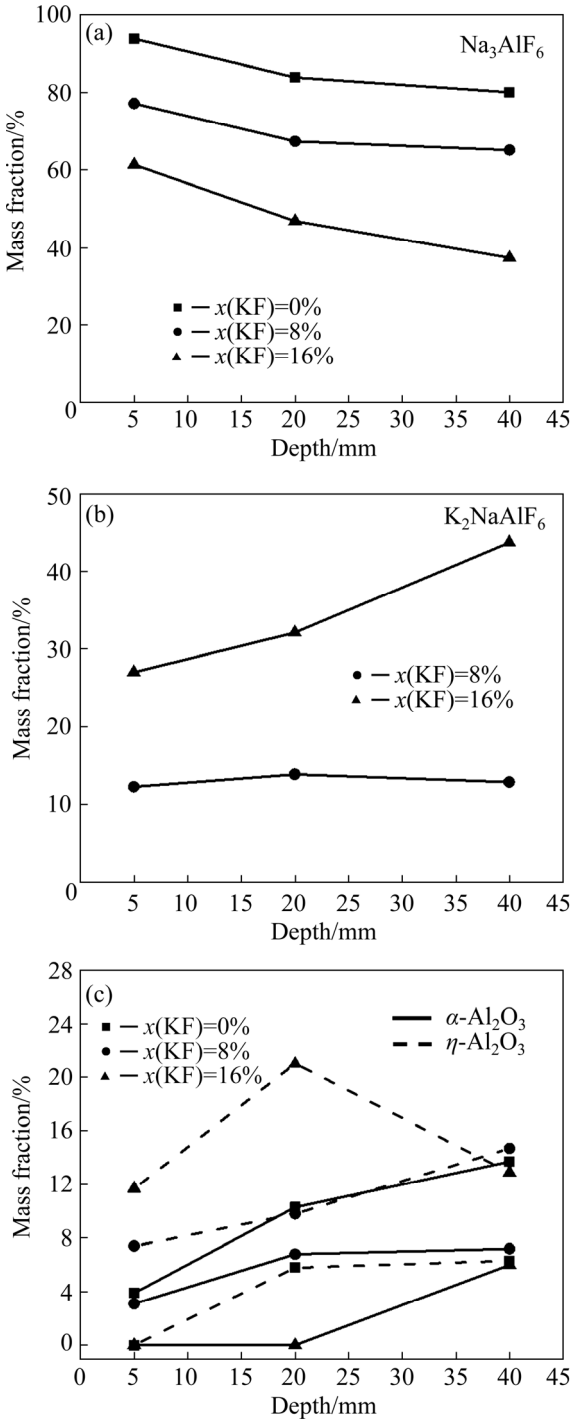

Fig. 5 Mass fractions of different phases in graphite cathode for NaF−KF−AlF_3 system

Considering the electrolysis duration, the K_2NaAlF_6 phase will eventually become the dominant compound upon long-term electrolysis. The reactions can generally be described as [20]

$$2Na_5Al_3F_{14}+2KF\rightarrow K_2NaAl_3F_{12}+3Na_3AlF_6 \quad (2)$$

$$Na_5Al_3F_{14}+4KF\rightarrow 2K_2NaAlF_6+Na_3AlF_6 \quad (3)$$

(with a large excess of KF)

$Na_5Al_3F_{14}$ is the most critical phase in the early stages of electrolysis for low KF concentrations. Due to the presence of KF, the activity of NaF increases, which will promote Reaction (1). The penetration of Na into the cathode promotes electrolyte penetration and causes Na_3AlF_6 to gradually replace $Na_5Al_3F_{14}$ as the main phase. This process is a forward process, which promotes the corrosion of the cathode.

Increasing K−GIC formation promotes the cathodic exfoliation corrosion as the content of KF increases, thereby promoting further penetration of the electrolyte. The melting temperature is low and will not affect penetration as much as $K_2NaAl_3F_{12}$. If K_2NaAlF_6 is the primary phase, the electrolyte at the bottom of the cathode may be solid, further preventing penetration of the electrolyte because the electrolysis temperature is lower than the melting temperature.

3.3.2 Effects of KF and LiF contents on mass gain for graphite cathode

To better understand the effects of LiF on electrolyte penetration, the Na_3AlF_6−LiF−AlF_3 system containing 4% KF was investigated. Upon adding LiF, the composition of the electrolyte after electrolysis is changed. NaF, Na_3AlF_6, KF, K_2NaAlF_6, LiF, K_2LiAlF_6, and two types of alumina are the main phases. Because of the decomposition of $Na_3Li_3Al_2F_{12}$ at 500−600 °C, the $Na_3Li_3Al_2F_{12}$ phase cannot be detected after calcination and LiF addition [23]. The change in composition contents is shown in Fig. 6.

As shown in Fig. 6(a), the Na_3AlF_6 content decreases with the increasing depth at x(LiF)=0 and 8%. However, it shows an increasing trend at x(LiF)=16%. The Na_3AlF_6 content reaches 90% for a depth of 40 mm. Figure 6(b) shows that the K_2NaAlF_6 content decreases with the increasing LiF content at the same depth. Figure 6(c) shows a relatively high LiF content in the middle of the

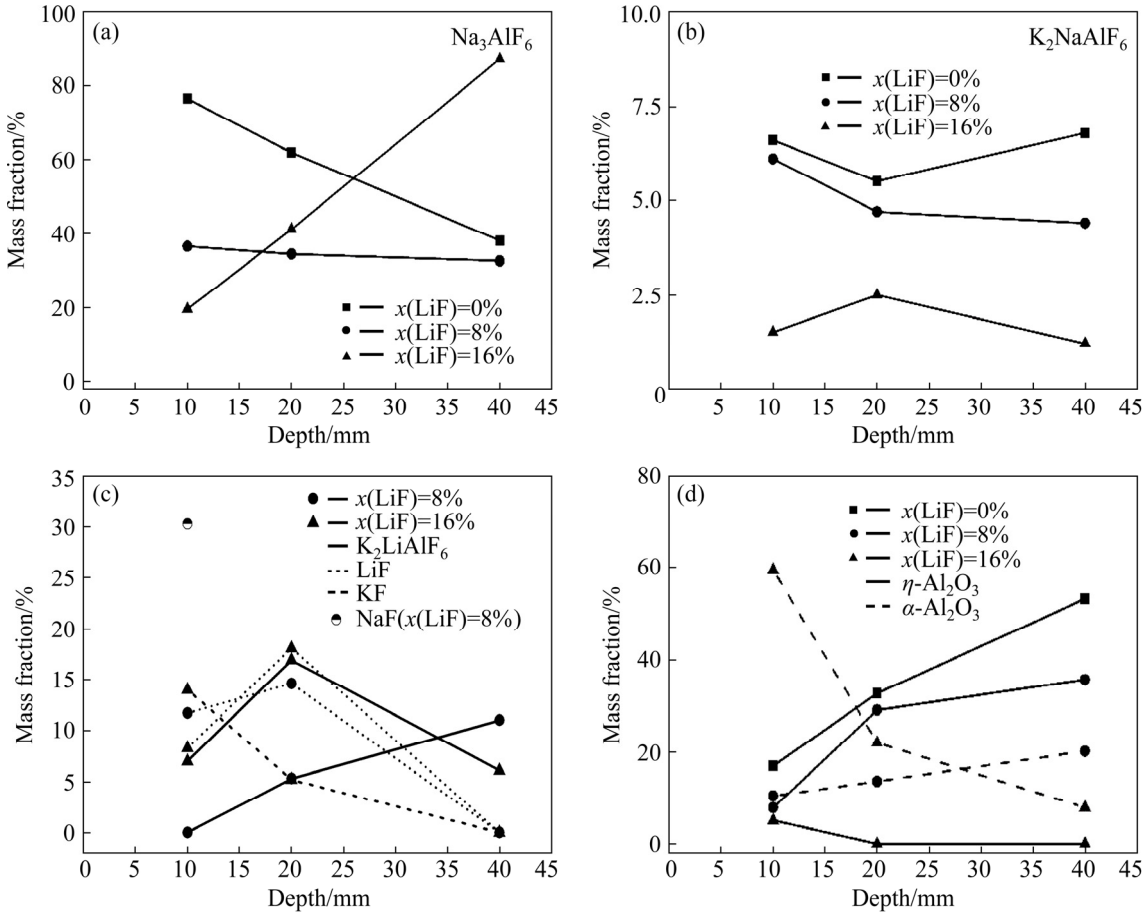

Fig. 6 Mass fractions of different phases at different depths of carbon cathode in NaF−4%KF−LiF−AlF_3 system

cathode compared with those at other depths. This is different from the penetration of KF and NaF or other phases without LiF. In addition, there is a high content of NaF and KF at the top of the cathode. For the K_2LiAlF_6 phase, the penetration behavior shows a different trend at x(LiF)=8% and x(LiF)=16%. As shown in Fig. 6(d), the transformation from α-Al_2O_3 to η-Al_2O_3 is hindered by increasing LiF content.

In combination with Fig. 2, it is found that LiF can alleviate electrolyte penetration, but only if the LiF content far exceeds the KF content. LiF is mainly in the form of the $Na_5Al_3F_{14}$ solid solution or K_2LiAlF_6 if LiF content is lower than KF. It does not play an essential role in the compounds. Therefore, it does little to alleviate electrolyte penetration. Conversely, LiF exists in the form of $Na_3Li_3Al_2F_{12}$ in the cathode and it plays an essential role in alleviating electrolyte penetration. As the Li content increases, the wetting angle of the electrolyte on the graphite cathode increases, which decreases capillary pressure, inhibits the wettability of the electrolyte melt to the graphite cathode, and hinders the electrolyte penetration [15].

LiF is converted directly into $Na_3Li_3Al_2F_{12}$ or $Na_5Al_3F_{14}$ in the cathode within a short period of time. Upon extended electrolysis with excessive NaF, $Na_5Al_3F_{14}$ is transformed into Na_3AlF_6 in the penetration process. Furthermore, a K_2LiAlF_6 phase is also produced in the process. The production of this phase is promoted in high-LiF and low-KF content systems. The $Na_3Li_3Al_2F_{12}$ phase is mainly accumulated in the upper part of the cathode, but the K_2LiAlF_6 and Na_3AlF_6 phases still penetrate to the bottom of the cathode. With the accumulation of LiF in the upper part of the cathode, $Na_3Li_3Al_2F_{12}$ can fill the pores and cracks of the cathode and effectively prohibit electrolyte penetration.

4 Conclusions

(1) The electrolyte compositions of cathodes before and after electrolysis were investigated by XRD and SEM. $Na_5Al_3F_{14}$, Na_3AlF_6, and K_2NaAlF_6 are the main phases in the electrolyte in NaF−KF−AlF_3 systems, while $Na_5Al_3F_{14}$ and $Na_3Li_3Al_2F_{12}$ are the main phases in the electrolytes of NaF−KF−LiF−AlF_3 systems with high LiF contents.

(2) In NaF−KF−AlF_3 systems, Na_3AlF_6 phase is produced, followed by $Na_5Al_3F_{14}$ phase upon the interaction of NaF and KF. $K_2NaAl_3F_{12}$ is also produced with increasing KF content in the penetrated electrolyte. Solid solutions containing KF or K_2NaAlF_6 can promote the electrolyte penetration.

(3) Low-content LiF does not affect electrolyte penetration in NaF−AlF_3 or NaF−KF−AlF_3 systems. For this system containing high-content LiF, $Na_3Li_3Al_2F_{12}$ and K_2LiAlF_6 are produced, followed by the $Na_5Al_3F_{14}$ phase. $Na_3Li_3Al_2F_{12}$ can effectively prohibit the electrolyte penetration, and the phase mainly exists in the upper part of the cathode.

(4) Based on our findings, an electrolyte system comprising $Na_5Al_3F_{14}$ solid solutions containing KF and $Na_3Li_3Al_2F_{12}$ may be optimal.

Acknowledgments

We acknowledge the financial supports from the National Natural Science Foundation of China (Nos. 51774080, 22078056), and the National Key R&D Program of China (No. 2018YFC1901905).

References

[1] SHE Xin-wei, JIANG Xian-quan, TAN Xiao-dong, GUO Sheng-feng, TANG Bin-bin, PAN Fu-sheng. Status and prospect for aluminum industrial development in China [J]. The Chinese Journal of Nonferrous Metals, 2020, 30: 709−718. (in Chinese)

[2] SLEPPY W C, COCHRAN C N. Bench scale electrolysis of alumina in sodium fluoride−aluminum fluoride melts below 900 °C [M]//Essential Readings in Light Metals. Hoboken, NJ, USA: John Wiely & Sons, Inc., 2013: 1089−1094.

[3] LIU Dong-ren, YANG Zhan-hong, LI Wang-xing. Electrochemical behavior of graphite in KF−AlF_3-based melt with low cryolite ratio [J]. Journal of the Electrochemical Society, 2010, 157: D417.

[4] FANG Zhao, DANG Yang-yang, PENG Jia-xin, HAN Ze-xun, MA Na-ni, LV Xiao-jun, LIU Man-bo, LI Lin-bo. Liquidus temperature of xNaF/AlF_3−Al_2O_3−CaF_2−MgF_2−KF−y($LiAlO_2$/LiF) molten salts energy system in aluminum electrolysis [J]. Nanoscience and Nanotechnology Letters, 2018, 10: 81−86.

[5] APISAROV A P, DEDYUKHIN A E, RED'KIN A A, TKACHEVA O Y, ZAIKOV Y P. Physicochemical properties of KF−NaF−AlF_3 molten electrolytes [J]. Russian Journal of Electrochemistry, 2010, 46: 633−639.

[6] KUBÍKOVÁ B, MLYNÁRIKOVÁ J, BOČA M, SHI Z N, GAO B L, PATEL N. Temperatures of primary crystallization and density of the KF + AlF_3 + LiF + Al_2O_3 molten system [J]. Journal of Chemical & Engineering Data, 2018, 63: 3047−3052.

[7] PENG Jian-ping, WEI Zheng, DI Yue-zhong, WANG

Yao-wu, SUN Ting. Alumina solubility in NaF−KF−LiF−AlF_3-based low-temperature melts [J]. JOM, 2020, 72: 239−246.

[8] YASINSKIY A, SUZDALTSEV A, PADAMATA S K, POLYAKOV P, ZAIKOV Y. Electrolysis of low-temperature suspensions: An update [M]//Light Metals 2020. Cham: Springer Nature Switzerland AG, 2020: 626−636.

[9] CUI P, SOLHEIM A, HAARBERG G M. The performance of aluminum electrolysis in cryolite based electrolytes containing LiF, KF and MgF_2 [C]//Light Metals 2015. Hoboken: John Wiley & Sons, Inc., 2015: 661−664.

[10] YAN Heng-wei, YANG Jian-hong, LI Wang-xing, CHEN Sha-zi. Alumina solubility in KF−NaF−AlF_3-based low-temperature electrolyte [J]. Metallurgical and Materials Transactions B, 2011, 42: 1065−1070.

[11] YAN Heng-wei, LIU Zhan-wei, MA Wen-hui, HUANG Li-qiang, WANG Cheng-zhi, LIU Ying-xin. KF−NaF−AlF_3 system: Liquidus temperature and phase transition [J]. JOM, 2020, 72: 247−252.

[12] FENG Nai-xiang. Penetration of cryolite melt and sodium into cathode carbon blocks during electrolysis [J]. Acta Metallurgica Sinica, 1999, 35: 611−617.

[13] FENG Nai-xiang. Aluminum electrolysis [M]. Beijing: Chemical Industry Press, 2006. (in Chinese)

[14] LIU Dong-ren, YANG Zhan-hong, LI Wang-xing, WANG Su-qin, WANG Shen-wei. Cathodic behavior of graphite in KF−AlF_3-based melts with various cryolite ratios [J]. Journal of Solid State Electrochemistry, 2011, 15: 615−621.

[15] ZHANG Yue-hong, ZHAI Xiu-jing, WANG Yao-wu, PENG Jian-ping, FENG Nai-xiang. Penetration of electrolyte containing KF and LiF into graphite cathode during aluminum electrolysis [J]. The Chinese Journal of Process Engineering, 2011, 11: 755−760. (in Chinese)

[16] CHEN Bing-xu, PENG Jian-ping, WANG Yao-wu, DI Yue-zhong. Study on liquidus temperature of NaF−KF−LiF−AlF_3 system with low cryolite ratio [J]. Metallurgical and Materials Transactions B, 2020, 51(3): 1181−1189.

[17] PADAMATA S K, YASINSKIY A S, POLYAKOV P V. Anodic process on Cu−Al alloy in KF−AlF_3−Al_2O_3 melts and suspensions [J]. Transactions of Nonferrous Metals Society of China, 2020, 30: 1419−1428.

[18] TAO Shao-hu, DI Yue-zhong, PENG Jian-ping, LIU Ke-jia, LI Ying-long, FENG Nai-xiang. Cathodic electrochemical behavior in Na_3AlF_6–Al_2O_3−LiF-based melts at tungsten electrode with various cryolite ratios [J]. Rare Metals, 2018, 37: 40−46.

[19] FANG Zhao, WU Xiao-lei, YU Juan, LI Lin-bo, ZHU Jun. Electrochemical insertion and penetration and migration behavior of alkali metal in aluminum electrolysis process [J]. The Chinese Journal of Nonferrous Metals, 2013, 23: 1746−1756. (in Chinese)

[20] KIRIK S D, ZAITSEVA Y N, LESHOK D Y, SAMOILO A S, DUBININ P S, YAKIMOV I S, SIMAKOV D A, GUSEV A O. NaF−KF−AlF_3 system: Phase transition in $K_2NaAl_3F_{12}$ ternary fluoride [J]. Inorganic Chemistry, 2015, 54: 5960−5969.

[21] SAMOILO A S, ZAITSEVA Y N, DUBININ P S, PIKSINA O E, RUZHNIKOV S G, YAKIMOV I S, KIRIK S D. Structural aspects of the formation of solid solutions in the NaF−KF−AlF_3 system [J]. Journal of Solid State Chemistry, 2017, 252: 1−7.

[22] FOSTER P A. Phase diagram of a portion of the system Na_3AlF_6−AlF_3−Al_2O_3 [J]. Journal of the American Ceramic Society, 1975, 58: 288−291.

[23] HOLM J L, HOLM B J, DANIELSSON B, HOLME D, LAMVIK A, SUNDE E L, SØRENSEN N A. Phase investigations in the system Na_3AlF_6–Li_3AlF_6 [J]. Acta Chemica Scandinavica, 1970, 24: 2535−2545.

低分子比 NaF−KF−LiF−AlF_3 体系电解质在石墨阴极中的渗透行为

陈炳旭，彭建平，王耀武，狄跃忠

东北大学 冶金学院，沈阳 110819

摘　要：研究分子比为 1.3 的 NaF−KF−LiF−AlF_3 体系电解质在石墨阴极中的渗透行为，通过 XRD 分析对电解前后阴极中的电解质进行系统研究，并通过 MUAD 的半定量计算对结果进行分析。结果表明，KF 可以促进电解质的渗透， KF 含量越高，渗透性越强。在电解质渗透过程中，K_2NaAlF_6 和含有 KF 的固溶体在含有 KF 的体系中发挥重要作用。LiF 有效地抑制电解质渗透，$Na_3Li_3Al_2F_{12}$ 相在高 LiF 含量的体系中发挥了重要作用。

关键词：铝电解；KF；LiF；阴极渗透；电解质成分；低分子比

(Edited by Xiang-qun LI)